Title

Longitudinal study using voxel-based relaxometry: Association between cartilage T1ρ and T2 and patient reported outcome changes in hip osteoarthritis

Journal

Journal of Magnetic Resonance Imaging, 45(5)

ISSN

1053-1807

Authors

Pedoia, Valentina
Gallo, Matthew C
Souza, Richard B
et al.

Publication Date

2017-05-01

DOI

10.1002/jmri.25458

Peer reviewed

HHS Public Access

Author manuscript

J Magn Reson Imaging. Author manuscript; available in PMC 2018 May 01.

Published in final edited form as:

J Magn Reson Imaging. 2017 May ; 45(5): 1523–1533. doi:10.1002/jmri.25458.

A longitudinal Study using voxel-based relaxometry: association between cartilage $T_{1\rho}$ and T_2 and patient reported outcome changes in hip osteoarthritis

Valentina Pedoia, PhD[1,*], **Matthew C. Gallo, BA**[1,*], **Richard B. Souza, PT, PhD**[1,2], and **Sharmila Majumdar, PhD**[1]

[1]Musculoskeletal Quantitative Imaging Research Group, Department of Radiology and Biomedical Imaging, University of California San Francisco, San Francisco, CA USA

[2]Department of Physical Therapy and Rehabilitation Science, University of California San Francisco, San Francisco, CA USA

Abstract

Purpose—To study the local distribution of hip cartilage $T_{1\rho}$ and T_2 relaxation times and their association with changes in patient reported outcomes (PROMs) using a fully automatic, local, and unbiased method in subjects with and without hip osteoarthritis (OA).

Materials and Methods—3T MRI studies of the hip were obtained for 37 healthy controls and 16 subjects with radiographic hip OA. The imaging protocol included a 3D SPGR sequence and a combined 3D $T_{1\rho}$ and T_2 sequence. Quantitative cartilage analysis was compared between a traditional region of interest (ROI)-based method and a fully automatic voxel-based relaxometry (VBR) method. Additionally, VBR was used to assess local $T_{1\rho}$ and T_2 differences between subjects with and without OA, and to evaluate the association between $T_{1\rho}$ and T_2 and 18-month changes PROMs.

Results—Results for the two methods were consistent in the acetabular (R=0.79, CV=2.9%) and femoral cartilage (R=0.90, CV=2.6%). VBR revealed local patterns of $T_{1\rho}$ and T_2 elevation in OA subjects, particularly in the posterosuperior acetabular cartilage ($T_{1\rho}$: p-value=0.02, T_2: p-value=0.038). Overall, higher $T_{1\rho}$ and T_2 values at baseline, particularly in the anterosuperior

Corresponding Author. Dr. Valentina Pedoia, MQIR, Department of Radiology and Biomedical Imaging, University of California, San Francisco, 1700 4th St., Suite 201, Box 2520, San Francisco, CA 94158, (Tel) 415-549-9242, (Fax) 415-514-9653, Valentina.Pedoia@ucsf.edu.

*Represents Equal Contribution as first author

Author Contributions

Study and Concept Design: all authors
Data Analysis and Results Interpretation: all authors
Statistical and Image Processing Expertise: VP
Manuscript Draft: MCG, VP
Critical Review, Edit and Proof of Manuscript: all authors
Obtaining of funding: RBS, SM
MCG and VP had full access to all of the data in the study and take full responsibility for the integrity of the data and the accuracy of the data analysis

Financial Interest

The authors certify that there are no conflicts of interest to report.

acetabular cartilage ($T_{1\rho}$: Rho=−0.42, p-value=0.002, T_2: Rho=−0.44, p-value=0.002), were associated with worsening PROMS at 18-month follow up

Conclusions—VBR is an accurate and robust method for quantitative MRI analysis in hip cartilage. VBR showed the capability to detect local variations in $T_{1\rho}$ and T_2 values in subjects with and without osteoarthritis, and voxel based correlations demonstrated a regional dependence between baseline $T_{1\rho}$ and T_2 values and changes in PROMs.

Keywords

$T_{1\rho}$; T_2; hip cartilage; osteoarthritis; voxel-based relaxometry; atlas-based segmentation

Introduction

Hip Osteoarthritis (OA) is a common, debilitating joint disease primarily characterized by articular cartilage degeneration (1). Traditionally, hip OA has been diagnosed with plain radiographs, but radiography provides an indirect assessment of cartilage degeneration and is insensitive to early disease processes (2). In the movement towards early diagnosis, biochemical or quantitative MRI techniques have shown great potential (2–5). This class of techniques, which includes $T_{1\rho}$ and T_2 relaxation time measurements, is sensitive and specific to changes in cartilage matrix composition that precede morphological change (6–8). Thus, $T_{1\rho}$ and T_2 relaxation time measurements can identify early degeneration before abnormalities are visualized with radiographs.

Previous in vivo studies in the hip have shown that higher $T_{1\rho}$ and T_2 values are associated with disease status (radiographic and MR-based) and MR-based disease progression (9,10), although the associations between these values and patient reported outcome measures (PROMs) have not been explored. In both studies referenced above, localized subregional analysis of $T_{1\rho}$ and T_2 values demonstrated a superior ability to characterize group differences compared to a global approach. These results support $T_{1\rho}$ and T_2 as biomarkers of OA-related cartilage degeneration and suggest that localized analysis improves the sensitivity of the techniques.

Quantitative MRI assessments require image post-processing and are traditionally addressed through region of interest (ROI)-based approaches (11). These approaches require trained users to manually or semi-automatically segment cartilage compartments (i.e. ROIs). These approaches are time-consuming, introduce user variability, and average all voxels in the ROI to compute the $T_{1\rho}$ or T_2 value. Multiple techniques have been proposed to overcome these limitations including the development of several automatic segmentation techniques (11). However, the local analysis of $T_{1\rho}$ and T_2 in the hip remains a significant challenge. Several techniques have been employed to reduce the size of ROIs to improve sensitivity including subregional analysis, laminar analysis, and texture analysis, and these techniques may lead to earlier identification of cartilage matrix changes (12,13). Yet these techniques do not address the segmentation challenge. Therefore, it is of great interest to find a technique that combines sensitive local analysis with automated segmentation.

Voxel-based relaxometry (VBR) is a technique that allows for the comparison of local differences in cartilage composition between two groups on a voxel-basis. $T_{1\rho}$ VBR was recently proposed for knee cartilage relaxation time analysis (14). This prior study demonstrated that VBR was feasible and consistent with traditional ROI-based analysis in the knee joint. VBR has also showed promising results in a study which evaluated the contribution of cartilage lesions to the longitudinal progression of $T_{1\rho}$ and T_2 after ACL reconstruction in a multi-center study (15).

Due to the shape of the hip joint, thinness of cartilage, and relatively low resolution of $T_{1\rho}$ images, the application of hip cartilage VBR poses an imaging challenge. Previous work has used VBR in the hip to complement a traditional ROI-based analysis[10]. However, neither a formal evaluation of the technique or uses beyond group analysis have been presented.

Accordingly, the aim of this study is threefold. (i) To evaluate the agreement between a VBR approach and an established ROI-based technique for the quantitative analysis of hip cartilage, considering the semi-automatic ROI-based method as a gold standard. To fulfill this aim we compared semi-automatic and automatic quantification of $T_{1\rho}$ and T_2 relaxation times using Coefficient of Variation (CVs) and Pearson correlation coefficients as metrics of the agreement between manual and automatic ROI-based results. Additionally an ad-hoc analysis studying the correlation between algorithm performances and KL grading was performed to prove the ability of the automatic method to handle cases characterized by highly degenerated cartilage.

(ii) To demonstrate both single patient and group applications of the VBR technique using voxel based Statistical Parametric Mapping (SPM) analysis. specifically we used local z-score conversion and analysis of the covariance (ANCOVA) linear model.

(iii) To use VBR to assess the local association between $T_{1\rho}$ and T_2 and change in PROMs over a period of time of 18 months using Spearman correlation SPM technique

We hypothesized that VBR is a feasible method for the fully automatic analysis of hip cartilage relaxation times; we expected a high correlation between manual and automatic ROI-based $T_{1\rho}$ and T_2 relaxation time quantification results. Moreover, we expected differences between the two techniques to be comparable with the inter-rater variation of the gold standard.

We also hypothesized that the local sensitivity of VBR reveals local patterns in single subject and group analysis as well as the local associations between relaxation times and PROMS, which are obscured by the averaging of a classical ROI-based approach.

Materials and Methods

Subjects

Hip MR images from 53 subjects, collected as part of an ongoing longitudinal study on hip OA, were assessed,. 37 subjects were classified as healthy controls [Kellgren-Lawrence (KL) grade ≤ 1] and 16 were classified as having mild or moderate hip OA (KL grade 2 or 3). Demographics information is reported in Table 1. All participants were between 23 and

69 years old and did not have: (i) history of hip surgery, (ii) knee OA with KL ≥ 2, (iii) hip KL of 4, (iv) any condition other than OA which could limit lower extremity function or mobility, and (v) MRI contraindications. As part of the procedure for this study, anterior-posterior, weight-bearing radiographs of the pelvis were obtained for all subjects at baseline; a board-certified musculoskeletal radiologist with 25 years of experience performed KL grading. All subjects provided informed consent prior to inclusion. The University Committee on Human Research approved this study.

MRI Protocol

All MR images were acquired using a 3 Tesla scanner (GE MR750; GE Healthcare, Waukesha, WI) using an 8-channel receive-only cardiac coil (GE Healthcare, Waukesha, WI). For all scans, the subject's feet were internally rotated and their forefeet were taped together to achieve a reproducible hip joint position. The MRI protocol included a 3D SPGR (MERGE) sequence for semi-automatic cartilage segmentation and a combined $T_{1\rho}$ and T_2 mapping sequence for cartilage composition assessment, the latter detailed by Li et al (16) (Table 2). Both sequences were scanned in the sagittal plane and were acquired with the same prescription.

Patient Reported Outcomes

Self-reported pain and function were assessed at baseline and 18-month follow up using the Hip Disability and Osteoarthritis Outcome Score (HOOS) (17). The HOOS covers five domains: pain, other symptoms, function during activities of daily living (ADL), function during sport and recreation (SPORT), and hip related quality of life (QOL). Percentage scores range from 0–100, with a lower HOOS score representing worse pain or function.

Image Processing

All image post processing was performed using an in-house software program developed in MATLAB (Mathworks Inc, El Segundo, CA) (18).

ROI-Based Method

MERGE images as well as all the $T_{1\rho}$- and T_2-weighted images were rigidly registered to the first $T_{1\rho}$-weighted image (TSL=0) using the VTK CISG Registration Toolkit (Kitware Inc, Clifton Park, NY). $T_{1\rho}$ and T_2 maps were then computed using voxel-based two-parameter exponential fitting ($S(TSL) \propto S_0 * \exp(-TSL/T_{1\rho})$ and $S(TE) \propto S_0 * \exp(-TE/T_2)$). The femoral and acetabular cartilage ROIs were segmented separately on the MERGE image using a semi-automated segmentation algorithm that relies on Bezier splines and edge detection (19). The two ROIs were segmented on approximately four slices near the center of the hip, as slices affected by partial volumes were excluded from the segmentation. Segmented ROIs were then superimposed onto the $T_{1\rho}$ and T_2 maps and values were computed as an average of all voxels within the ROIs.

Voxel-Based Relaxometry (VBR) Method

Voxel-Based Relaxometry (VBR) is based on the registration of all the subjects on a unique space to allow for the comparison of similar anatomic locations on a voxel basis (20). A

single reference subject was selected through an iterative process aimed to minimize global deformation (i.e. Minimum Deformation Template (MDT)). Due to morphological differences across subjects, a non-rigid registration procedure was adopted to accomplish this task. The Elastix Toolbox was used to develop the registration (21). The advantage of using Elastix is the modular aspect of the library that allows for building highly efficacious algorithms. All the basic steps of a classical registration pipeline can be customized to select the best combination of image similarity metric, optimization algorithm, and interpolation strategy. Multiresolution hierarchical approaches are available, which allows for a balance between algorithm performance and execution time demands. The registration was carried out through an iterative process in the context of a minization framework. Good initialization is extremely critical for a correct convergence of the algorithm in the attempt to avoid local minima. The initialization procedure was based on Hugh transform that was employed to identify the femoral head centers in the MDT reference image and in each subject image. Hugh transform (22,23) is a well known computer vision method for object detection based on the transformation of all the points in the image in a parameter space defined by a specific equation; in our application the equation is a circle representing the section of the femoral head in each 2D slice.

$$(\mathrm{x}-\mathrm{C_x})^2-(\mathrm{y}-\mathrm{C_y})^2=\mathrm{R}^2$$

Where *[Cx,Cy]* are the coordinate of the femoral head center and *R* the ratio.

In the 3D parametric space *[Cx,Cy,R]* each point (x, y) on the perimeter of a circle will produce a cone surface. The triplet *(Cx, Cy, R)* corresponds to the 3D point where the largest number of cone surfaces intersects. Circle detection via Hugh transform was performed in six central slices and the slice with the biggest detected circle is used to identify Cz.

Due to the high anisotropy of the voxels [0.5 × 0.5 × 4 mm], a 2D method was prefered to a 3D sphere detection approach.

The translation vector *T=[tx,ty,tz]* that overlaps the MDT and each subject centers was applied as initialization of the registration procedure.

After initialization, a five level recursive pyramidal multi-resolution with random sampler approach was used to estimate the non-rigid transformation. The semiautomatic ROIs identified on the reference image were then used to constrain a second iteration of the registration procedure targeted to perform just in the cartilage region. The non-rigid registration technique was applied between the reference and each of the 1st TSL = 0, $T_{1\rho}$-weighted image. The transformation field obtained is then applied on all the later TLS images.

$T_{1\rho}$ maps were obtained by fitting the morphed T1ρ-weighted images obtained with different TSLs using a Levenberg-Marquardt mono-exponential ($S(TSL) \propto \exp(-TSL/T_{1\rho})$) applied on each voxel. T_2 maps were obtained with an identical process. The reference ROIs were then applied on the morphed maps, setting in this way a fully automatic, single atlas-

based segmentation allowing for comparison with the classical semiautomatic ROI-based method.

Statistical Analysis

The first set of experiments was aimed to validate the fully automatic technique proposed in this paper. ROI-based results for the automatic method were evaluated against the semiautomatic method using mean $T_{1\rho}$ values and standard deviations, average of each case's coefficient of variation (CV), absolute $T_{1\rho}$ differences, and Pearson correlation coefficients; comparisons were made separately in the acetabular and femoral cartilage ROIs. Additionally, Spearman correlation coefficients were computed between CV and KL grade to assess algorithm performance at different disease states. Analyses were run in the overall cohort as well as in the control and osteoarthritis groups.

Because the registration was based on the TE/TSL = 0 image, which in our combined sequence (16) was considered for both $T_{1\rho}$ and T_2 maps fitting, the algorithm performance were evaluated just for $T_{1\rho}$.

A second set of experiments was performed to demonstrate the application of single subject and group. As an example of usage of the proposed technique, VBR was used to normalize $T_{1\rho}$ values in a single KL grade 3 subject (61 year-old male, BMI 27.3 kg/m^2) using 14 KL grade 0 subjects as reference (average age 41 years, 10 females, average BMI 24.1 kg/m^2). Z-score SPM was used to study local $T_{1\rho}$ abnormality, and was computed as follows:

$$Z(x,y,z)=\frac{T_{1\rho}(x,y,z)-\overline{T_{1\rho}}_{KL=0}(x,y,z)}{\sigma T_{1\rho}{}_{KL=0}(x,y,z)}$$

Where $T_{1\rho}(x,y,z)$ is the $T_{1\rho}$ value in the point (x,y,z), $\overline{T_{1\rho}}_{KL=0}(x,y,z)$ and $\sigma T_{1\rho\ KL=0}(x,y,z)$ are the mean and standard deviation $T_{1\rho}$ computed across the 14 KL 0 control subjects in the same (x,y,z) location.

For group VBR, all $T_{1\rho}$ and T_2 relaxation time maps in the dataset were analyzed to extract mean and standard deviation for each voxel across the OA and control groups. Voxel-based analysis of covariance (ANCOVA) linear model was used to assess group differences and the resulting p-values were used to create volumetric SPMs. $P < 0.05$ was set as the level of significance. OA group was observed to be significant older (KL 0–1 age [23,69] and KL>1 age [29,71]. This effect was removed from our analysis by considering age as a covariate in the model.

Spearman correlation was used to assess the ability of baseline $T_{1\rho}$ and T_2 to predict the change in patient reported outcome (HOOS) over 18 months. VBR was used to build Rho value SPMs, which allow for exploring local associations.

Statistical Parametric Maps 3D Visualization

3D visualization of the SPMs was generated using a technique based on Laplace's equation previously used to generate cartilage thickness maps (24). The technique yields a one-to-one

matching between points in the bone-cartilage interface and points in the articular surface with no crossings. Laplace's equation was numerically solved in three dimensions with Dirichlet boundary conditions to obtain a potential map. A vector field was generated to lead each point in the bone cartilage interface to a point in the articular surface. Average values along this trajectory were computed and projected on the triangulated mesh obtained from 3D bone segmentation of the reference hip.

Results

Fully Automatic ROI-based $T1_\rho$ Assessment

A qualitative assessment of the morphed map reveals that the local spatial distribution of $T1_\rho$ values is well-preserved; no major alterations – potentially caused by registration errors or interpolation issues – were noted. An original and morphed $T1_\rho$ map from a representative subject is shown in Figure 1.

Automatic and semiautomatic $T_{1\rho}$ quantification results were highly correlated (R = 0.79 and R = 0.90 in the acetabular and femoral cartilage, respectively). In the overall cohort, average CVs in the acetabular and femoral ROIs were 2.9 ± 2.9% and 2.6 ± 2.4%, respectively. Spearman correlations in the overall cohort showed no association between KL grade and algorithm performance (CV) in the acetabular (Rho = 0.06, p-value = 0.70) or femoral cartilage (Rho = −0.06, p-value = 0.67). Similar results were found when the analyses were repeated in the control and OA groups (Table 3). Both automatic and semiautomatic approaches showed higher $T_{1\rho}$ values in the acetabular cartilage in the OA group (semiautomatic: 33.37 ± 2.92 ms vs. 34.20 ± 2.93; automatic: 32.66 ± 2.85 vs. 33.72 ± 2.99 ms), but these differences did not reach significance.

VBR Single Subject Analysis

The results of the single subject analysis are shown in Figure 2. The z-score spatial distribution between the two groups is shown in Figure 2 (right), which is used to explore similarities or differences between $T_{1\rho}$ values in the KL 3 subject and the group mean of the KL 0 subjects. VBR analysis demonstrates local areas of z-score elevation in the OA subject: the posterosuperior and anterior femoral cartilage show elevation, as well as the posterior and superior acetabular cartilage. It is important to note that this technique allows us to visualize the spatial distribution of these differences.

VBR Group Analysis

Figure 3 shows the 3D visualization of the average voxel-based $T_{1\rho}$ maps for the OA and control groups. The average $T_{1\rho}$ maps show values in the expected range for both OA and control subjects: for OA subjects, global acetabular and femoral ROI averages of 33.7 and 35.7 ms, respectively; for control subjects, global acetabular and femoral ROI averages of 32.7 and 35.2 ms, respectively. Figure 4 shows the 3D visualizations of the T_2 maps. For OA subjects, global acetabular and femoral ROI averages were 27.4 and 30.8 ms, respectively; for control subjects, global acetabular and femoral ROI averages were 27.0 and 31.1 ms, respectively. It is worth noting how the 3D representations clearly show the local heterogeneity of the cartilage $T_{1\rho}$ and T_2 values.

Although the regression model adjusted by age revealed no significant differences between OA and controls groups for global acetabular (p-value = 0.31) or femoral (p-value = 0.72) $T_{1\rho}$ values, the analysis of the local differences reveals that the OA group had significant local $T_{1\rho}$ elevation compared to controls, primarily in the posterosuperior acetabular cartilage. No significant cluster of significant voxels is observed in the femoral cartilage. Figure 3 (right) shows the 3D reconstruction of the $T_{1\rho}$ p-value SPM. For T_2, similarly no significant differences between OA and controls for either the global acetabular (p-value = 0.78) or femoral (p-value = 0.65) cartilage. Local differences were located in similar area to $T_{1\rho}$, however the significant cluster was observed to be smaller (Figure 4).

Local association with ΔHOOS

In the global ROIs, no significant associations were found between baseline $T_{1\rho}$ or T_2 values and 18-month change in HOOS subscores. In the acetabular cartilage, $T_{1\rho}$ and T_2 values were not associated with changes in HOOS pain ($T_{1\rho}$: Rho = −0.15, p-value = 0.31; T_2: Rho = −0.06, p-value = 0.70), symptoms ($T_{1\rho}$: −0.14, 0.32; T_2: −0.16, 0.28), ADL ($T_{1\rho}$: 0.07, 0.65; T_2: −0.01, 0.97), SPORT ($T_{1\rho}$: −0.09, 0.54; T_2: −0.14, 0.34), or QOL ($T_{1\rho}$: −0.17, 0.25; T_2: −0.23, 0.11); in the femoral cartilage, $T_{1\rho}$ and T_2 values were not associated with changes in HOOS pain ($T_{1\rho}$: Rho = 0.03, p-value = 0.85; T_2: Rho = 0.13, p-value = 0.38), symptoms ($T_{1\rho}$: −0.03, 0.86; T_2: −0.02, 0.88), ADL ($T_{1\rho}$: 0.15, 0.30; T_2: 0.18, 0.21), SPORT ($T_{1\rho}$: 0.13, 0.37; T_2: 0.06, 0.67), or QOL ($T_{1\rho}$: −0.07, 0.61; T_2: 0.03, 0.82). However, local associations were observed through VBR analysis.

Figure 5 shows the 3D visualization of the voxel-based correlations between baseline $T_{1\rho}$ values in the acetabulum and change in HOOS SPORT. The correlation map shows that weak to moderate negative correlations are present in the anterosuperior acetabular cartilage. When the ROI is constrained to the anterosuperior acetabular cartilage, as seen in the Figure 5, average $T_{1\rho}$ values within the ROI demonstrate a significant negative correlation with delta HOOS SPORT (Rho = −0.42, p-value = 0.002), indicating that higher $T_{1\rho}$ values at baseline are associated with worse function during sports and recreational activities 18 months later. Moreover, the domains of pain (Rho = −0.31, p-value = 0.03), symptoms (−0.41, 0.005), ADL (−0.33, 0.02), and QOL (−0.32, 0.02) also showed significant negative associations when $T_{1\rho}$ was evaluated in the same anterosuperior acetabular cartilage ROI. Similarly, T_2 values showed an association with all HOOS domains within this ROI (Rho ranging between −0.439 and −0.29; p-value ranging between 0.002 and 0.03). No significant associations were found in the femoral cartilage for $T_{1\rho}$ or T_2.

Discussion

In this study we present and validate a novel automatic method for the analysis of MR $T_{1\rho}$ and T_2 relaxation time measurements in hip cartilage. This method combines an automatic, atlas-based segmentation and VBR, allowing for either a classical ROI-based analysis or a voxel-based analysis of cartilage biochemical composition in the hip. For ROI-based $T_{1\rho}$ quantification, we found a strong agreement between the automatic and semiautomatic segmentation method.. Further, algorithm performance was not associated with KL grade, supporting its use in healthy and OA populations. The results of the VBR technique were

promising. OA subjects demonstrated local $T_{1\rho}$ and T_2 elevation – particularly in the posterosuperior acetabular cartilage – that are in concordance with previously published literature using subregional ROI-based analysis (9). Taken together, these findings suggest that the method presented in this study is accurate and robust to different OA levels.

Results of our study add to current knowledge regarding atlas-based methods for local cartilage analysis. In this study, we extend a method developed for knee cartilage by Pedoia and colleagues (14) and optimize its application for hip cartilage. Compared with the knee joint, hip cartilage is much thinner, with an average thickness of 1.4 mm and 1.2 mm for the femoral and acetabular plates, respectively (25). Moreover, due to the high curvature of the cartilage, the large majority of the voxels that compose the cartilage are severely affected by partial volume effect. An ad-hoc procedure based on circle detection via generalized Hugh transform was adopted in this study prior to the application of the non-rigid registration. This initialization was a critical step in the overall procedure.

Similar to Pedoia et al.[14], our method uses the relatively low resolution and highly anisotropic $T_{1\rho}$ -weighted images to accomplish the registration task. Siversson et al. (26) previously proposed the use of a multi-atlas approach for the automatic morphological and biochemical assessment of the hip cartilage using TrueFISP dGEMRIC showing excellent results. However, this technique was evaluated on a relative small sample (15 subjects with mild or no radiographic osteoarthritis) and it used isotropic high-resolution images 0.6 mm^3.

In the current study, despite the use of the anisotropic and low resolution $T_{1\rho}$-weighted images for registration, the automatic segmentation showed strong agreement with the semiautomatic method in the acetabular and femoral cartilage in a larger sample (53 subjects) with a broad variation in disease status (KL grades 0–3).

The performances of the proposed algorithm were evaluated in terms of agreement with a semi-automatic method that involved extensive user manual intervention. It is worth noting that even if the comparison with human user is the most widely adopted practice in image segmentation, this gold standard method is affected by intra and inter-rater reliability and the algorithm performances need to be consider with this in mind. The agreement between automatic and semiautomatic procedures is comparable to the one obtained by two trained users segmenting the dataset with the semiautomatic method: inter-rater reliability was calculated in a subset of five patients in this study and CVs in the acetabular and femoral ROIs were 1.92% and 2.65%, respectively. Multiple users are common in studies with large enrollments or with longitudinal designs; the extensive training and error rate associated with such a time-consuming task could introduce bias in the data, leading to an misguided interpretation of. results. Considering OA related expectable changes, a previous study (10) showed an average 8.38% % and 6.97% $T_{1\rho}$ prolongation in the posterosuperior, and anterior femoral compartment in subjects that showed incident cartilage lesion 18 month later, suggesting that the VBR method presented in this study would be appropriate to detect changes of the same order. Additionally, similar performance across different KL grading is observed in this study, showing how the algorithm performs equally well across the whole disease spectrum.

To the best of our knowledge this is the first study to propose a fully automatic procedure for the analysis of the hip $T_{1\rho}$ and T_2 relaxation times.

Single-subject VBR demonstrates a novel application of this technique for individual patient assessment. In this study we compared cross sectional differences between a single OA subject and a group of KL 0 controls using z-score analysis. The z-score conversion normalizes the $T_{1\rho}$ values in the OA subject to the mean values of the control subjects in each voxel, allowing us to visualize areas of significant difference. For example, the OA subject had marked z-score elevation in the superior acetabular cartilage, which may have been overlooked on a purely qualitative assessment of the subject's $T_{1\rho}$ map. The ability to automatically characterize individual patient differences represents an essential step in the clinical translation of quantitative imaging and the movement towards precision medicine.

The results of the VBR group analysis are in agreement with those presented by Wyatt et al (9). In that study, a ROI-based method was used to assess differences in $T_{1\rho}$ and T_2 values between OA and control subjects (84 subjects total); no differences were noted in the global acetabular or femoral ROIs, but subregional analysis revealed that OA subjects had higher $T_{1\rho}$ and T_2 values in the posterosuperior acetabular cartilage, with $T_{1\rho}$ showing greater group differences. VBR results from our study confirm these findings, with the added benefit of fully visualizing the distribution of focal $T_{1\rho}$ elevation as the technique is not constrained by the a priori division of subregions; this may indicate that VBR is more sensitive to detecting local differences in cartilage composition and can identify features potentially masked by the averaging of a ROI-based subregional approach. In addition to sensitivity, VBR may provide greater objectivity in cartilage composition assessment. The a priori division of cartilage into subregions is typically based on the manual identification of anatomical landmarks and is therefore affected by inter- and intra-user variation. This could increase the chance of comparing different cartilage locations across subjects, or across time points. The non-rigid image registration used in VBR, however, allows for comparisons of the same anatomical areas across subjects, thereby accounting for local spatial variations due to the normal heterogeneity of the cartilage matrix, common loading pattern, or technical issues such as magic angle effect.

VBR revealed a regional association between $T_{1\rho}$ and T_2 values in the acetabulum and changes in HOOS scores over 18 months: worse cartilage composition in the anterosuperior acetabulum, measured as a higher $T_{1\rho}$ or T_2 value, was associated with detrimental changes in patient pain and/or symptoms. Although a previous study has described the association between higher $T_{1\rho}$ and T_2 and morphological progression in the hip (10), this is the first study to identify a relationship between quantitative imaging and changes in PROMs. Additionally, our findings suggest that the anterosuperior acetabular cartilage may be an important region to monitor in OA disease progression. This finding is supported by two sets of results: (i) a study by Kumar et al. (27) that demonstrated a strong association between acetabular cartilage lesions and PROMs and (ii) studies which have reported a high prevalence of cartilage lesions in the anterosuperior acetabular cartilage in subjects with hip OA (28,29).

Despite the promising results, there are several limitations of this study, including the relatively small sample size. Larger sample and multicenter studies are desirable for a more accurate validation of the technique that is an inevitable step before a possible distribution of the software. The complexity of the image-processing pipeline needs to be acknowledged as a limitation in terms of results' replication from other centers. Additionally, radiographic OA was defined only based on KL grade, as it is the most common definition of OA. Definitions based on MRI or clinical findings may have led to different results. Segmentation performance could be improved by using multi-atlas or multi-spectral approaches. While evidences of bi-exponential components in the cartilage tissue are shown in previous literature (30,31), the limited number of echoes (N=4) acquired our combined $T_{1\rho}/T_2$ sequence imposed the usage of a simple mono-exponential two parameters model, Keeping in mind the clinical translation of those techniques, in the future, fast acquisition techniques such as compressed sensing could make feasible the implementation of an in-vivo protocol that could allow for the acquisition of a larger number of echoes. In turn, this could open possibility for a more complex multi-component model and still satisfy the scan time constrains.

In conclusion, creating a single subject atlas and using VBR is an accurate and robust method for the local analysis of hip cartilage composition. VBR can provide an automatic, unbiased, and local assessment of group differences or it can be used to characterize a single subject. Moreover, VBR may improve the clinical translation of $T_{1\rho}$ relaxation time measurements due to its automated post-processing pipeline.

Acknowledgments

The authors would like to thank Thomas M. Link, MD, PhD, Cory Wyatt, PhD, and Deepak Kumar, PT, PhD for their contributions. The authors would also like to thank Melissa Guan for her help in recruiting and consenting patients.

Grant Support

This study was supported by the National Institute of Arthritis and Musculoskeletal and Skin Diseases, part of the National Institutes of Health, under Award Numbers NIH NIAMS P50 AR060752. The content is solely the responsibility of the authors and does not necessarily represent the official views of the National Institutes of Health.

References

1. Martel-Pelletier J. Pathophysiology of osteoarthritis. Osteoarthritis and Cartilage. 1998; 6(6):374–376. [PubMed: 10343769]
2. Gold GE, Cicuttini F, Crema MD, et al. OARSI Clinical Trials Recommendations: Hip imaging in clinical trials in osteoarthritis. Osteoarthritis and Cartilage. 2015; 23(5):716–731. [PubMed: 25952344]
3. Burstein D, Gray ML. Is MRI fulfilling its promise for molecular imaging of cartilage in arthritis? Osteoarthritis and Cartilage. 2006; 14(11):1087–1090. [PubMed: 16901724]
4. Roemer FW, Crema MD, Trattnig S, Guermazi A. Advances in Imaging of Osteoarthritis and Cartilage. Radiology. 2011; 260(2):332–354. [PubMed: 21778451]
5. Li X, Majumdar S. Quantitative MRI of articular cartilage and its clinical applications. Journal of magnetic resonance imaging : JMRI. 2013; 38(5):991–1008. [PubMed: 24115571]
6. Li N, Mangini J, Bhawan J. New prognostic factors of cutaneous melanoma: a review of the literature. Journal of cutaneous pathology. 2002; 29(6):324–340. [PubMed: 12135463]

7. Duvvuri U, Goldberg AD, Kranz JK, et al. Water magnetic relaxation dispersion in biological systems: The contribution of proton exchange and implications for the noninvasive detection of cartilage degradation. Proceedings of the National Academy of Sciences. 2001; 98(22):12479–12484.
8. Li X, Benjamin Ma C, Link TM, et al. In vivo T(1rho) and T(2) mapping of articular cartilage in osteoarthritis of the knee using 3 T MRI. Osteoarthritis Cartilage. 2007; 15(7):789–797. [PubMed: 17307365]
9. Wyatt C, Kumar D, Subburaj K, et al. Cartilage T1rho and T2 Relaxation Times in Patients With Mild-to-Moderate Radiographic Hip Osteoarthritis. Arthritis Rheumatol. 2015; 67(6):1548–1556. [PubMed: 25779656]
10. Gallo MC, Wyatt C, Pedoia V, et al. T1rho and T2 relaxation times are associated with progression of hip osteoarthritis. Osteoarthritis Cartilage. 2016
11. Pedoia V, Majumdar S, Link TM. Segmentation of joint and musculoskeletal tissue in the study of arthritis. Magma (New York, NY). 2016; 29(2):207–221.
12. Subburaj K, Valentinitsch A, Dillon AB, et al. Regional variations in MR relaxation of hip joint cartilage in subjects with and without femoralacetabular impingement. Magnetic resonance imaging. 2013; 31(7):1129–1136. [PubMed: 23684960]
13. Carballido-Gamio J, Stahl R, Blumenkrantz G, Romero A, Majumdar S, Link TM. Spatial analysis of magnetic resonance T1rho and T2 relaxation times improves classification between subjects with and without osteoarthritis. Medical physics. 2009; 36(9):4059–4067. [PubMed: 19810478]
14. Pedoia V, Li X, Su F, Calixto N, Majumdar S. Fully automatic analysis of the knee articular cartilage T1ρ relaxation time using voxel-based relaxometry. Journal of Magnetic Resonance Imaging. 2016; 43(4):970–980. [PubMed: 26443990]
15. Russell C, Pedoia V, Amano K, Potter H, Majumdar S. Consortium A-A. Baseline cartilage quality is associated with voxel-based T and T following ACL reconstruction: A multicenter pilot study. Journal of orthopaedic research : official publication of the Orthopaedic Research Society. 2016
16. Li X, Wyatt C, Rivoire J, et al. Simultaneous acquisition of T1rho and T2 quantification in knee cartilage: repeatability and diurnal variation. Journal of magnetic resonance imaging : JMRI. 2014; 39(5):1287–1293. [PubMed: 23897756]
17. Bagga D, Modi S, Poonia M, et al. T2 relaxation time alterations underlying neurocognitive deficits in alcohol-use disorders (AUD) in an Indian population: A combined conventional ROI and voxel-based relaxometry analysis. Alcohol. 2015; 49(7):639–646. [PubMed: 26537482]
18. Carballido-Gamio, J., Bauer, JS., Keh-Yang, L., Krause, S., Majumdar, S. Combined Image Processing Techniques for Characterization of MRI Cartilage of the Knee; Engineering in Medicine and Biology Society, 2005 IEEE-EMBS 2005 27th Annual International Conference of the; 2005. p. 3043-3046.
19. Carballido-Gamio J, Link TM, Li X, et al. Feasibility and reproducibility of relaxometry, morphometric, and geometrical measurements of the hip joint with magnetic resonance imaging at 3T. Journal of magnetic resonance imaging : JMRI. 2008; 28(1):227–235. [PubMed: 18581346]
20. Pell GS, Briellmann RS, Waites AB, Abbott DF, Jackson GD. Voxel-based relaxometry: a new approach for analysis of T2 relaxometry changes in epilepsy. NeuroImage. 2004; 21(2):707–713. [PubMed: 14980573]
21. Klein S, Staring M, Murphy K, Viergever MA, Pluim JP. elastix: a toolbox for intensity-based medical image registration. IEEE transactions on medical imaging. 2010; 29(1):196–205. [PubMed: 19923044]
22. Tsuji S, Matsumoto F. Detection of Ellipses by a Modified Hough Transformation. Ieee T Comput. 1978; 27(8):777–781.
23. Duda RO, Hart PE. Use of Hough Transformation to Detect Lines and Curves in Pictures. Commun Acm. 1972; 15(1):11-&.
24. Carballido-Gamio J, Majumdar S. Atlas-based knee cartilage assessment. Magnetic resonance in medicine. 2011; 66(2):574–583. [PubMed: 21773988]
25. Xia Y, Chandra SS, Engstrom C, Strudwick MW, Crozier S, Fripp J. Automatic hip cartilage segmentation from 3D MR images using arc-weighted graph searching. Physics in medicine and biology. 2014; 59(23):7245–7266. [PubMed: 25383566]

26. Siversson C, Akhondi-Asl A, Bixby S, Kim YJ, Warfield SK. Three-dimensional hip cartilage quality assessment of morphology and dGEMRIC by planar maps and automated segmentation. Osteoarthritis Cartilage. 2014; 22(10):1511–1515. [PubMed: 25278060]

27. Kumar D, Wyatt CR, Lee S, et al. Association of cartilage defects, and other MRI findings with pain and function in individuals with mild-moderate radiographic hip osteoarthritis and controls. Osteoarthritis Cartilage. 2013; 21(11):1685–1692. [PubMed: 23948977]

28. Teichtahl AJ, Wang Y, Smith S, et al. Structural changes of hip osteoarthritis using magnetic resonance imaging. Arthritis Research & Therapy. 2014; 16(5):466. [PubMed: 25304036]

29. Nepple JJ, Carlisle JC, Nunley RM, Clohisy JC. Clinical and radiographic predictors of intra-articular hip disease in arthroscopy. The American journal of sports medicine. 2011; 39(2):296–303. [PubMed: 21098820]

30. Reiter DA, Lin PC, Fishbein KW, Spencer RG. Multicomponent T2 relaxation analysis in cartilage. Magnetic resonance in medicine. 2009; 61(4):803–809. [PubMed: 19189393]

31. Magin RL, Li W, Pilar Velasco M, et al. Anomalous NMR relaxation in cartilage matrix components and native cartilage: fractional-order models. Journal of magnetic resonance. 2011; 210(2):184–191. [PubMed: 21498095]

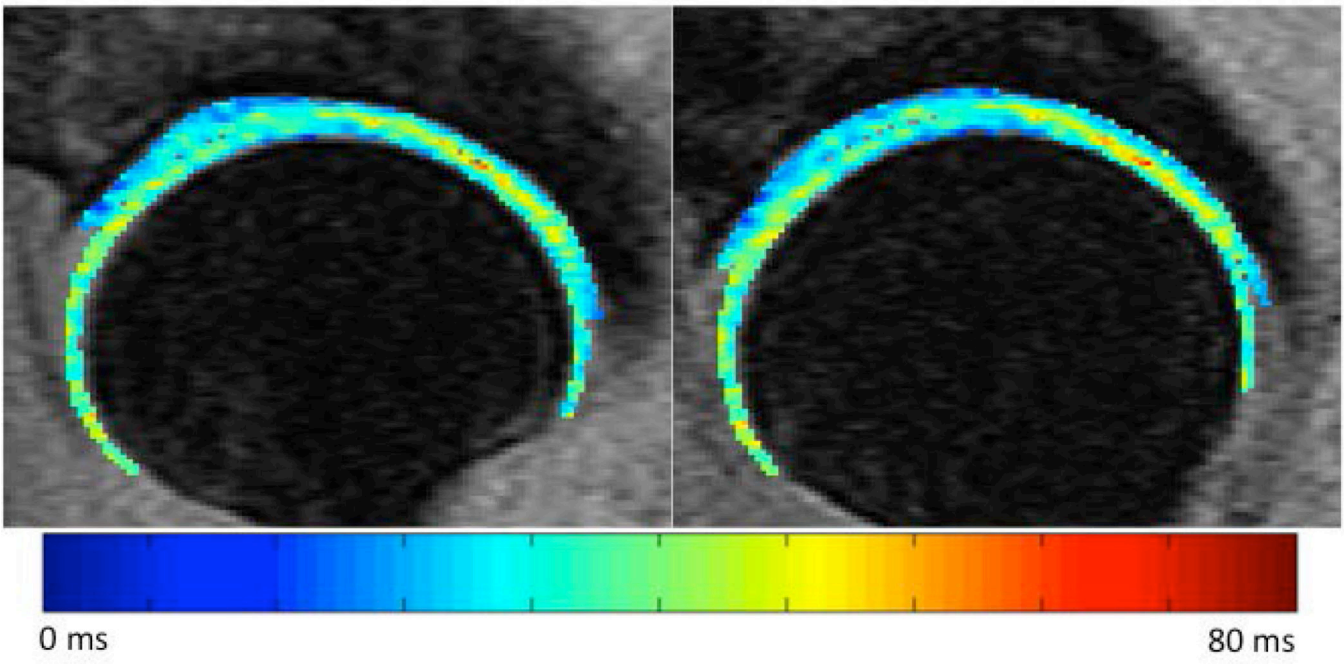

Figure 1.
Original (left) and morphed (right) $T_{1\rho}$ map of a 51 year-old female subject (KL grade 1).

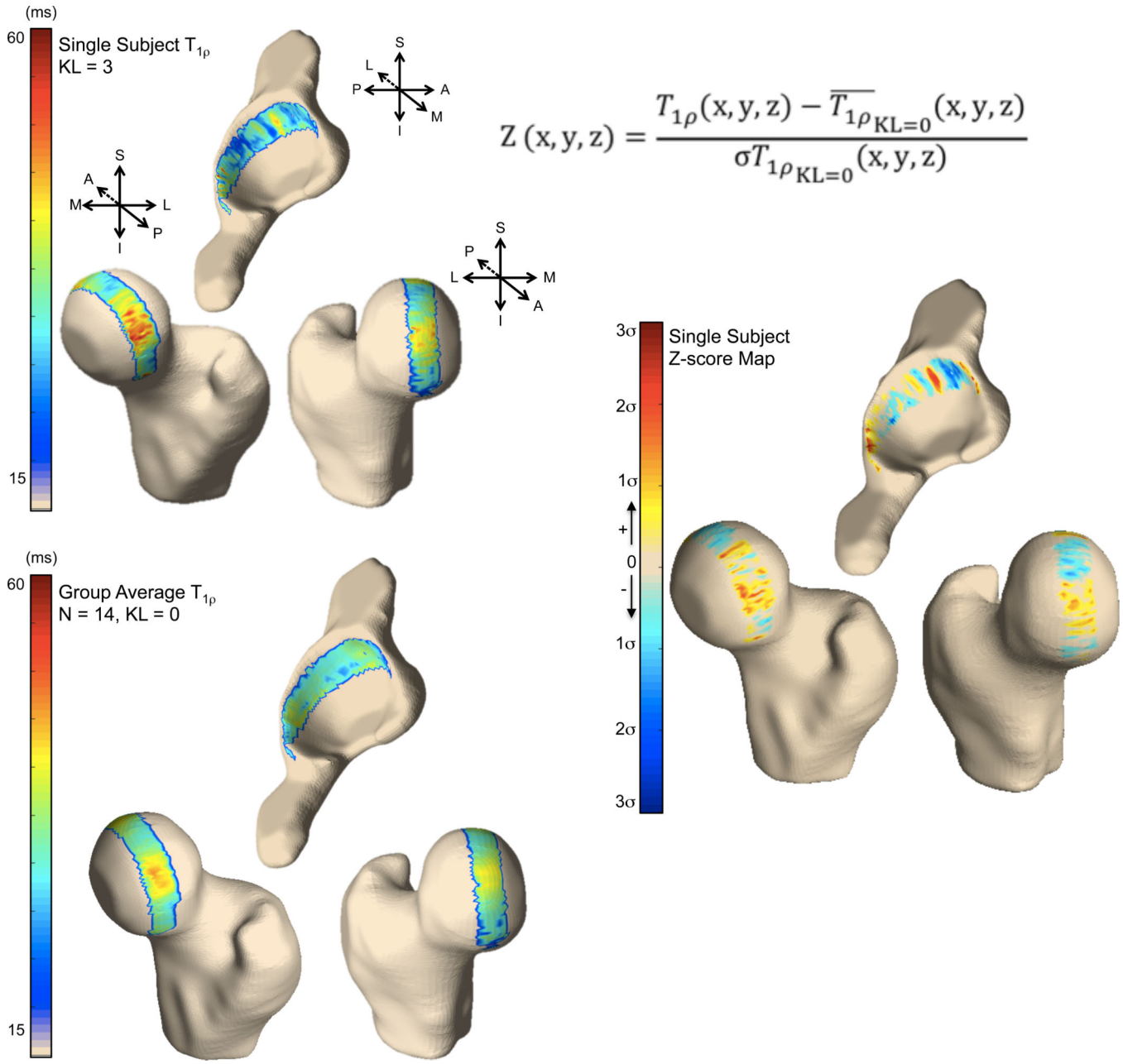

Figure 2.

3D visualization of the voxel-based $T_{1\rho}$ maps for a single OA subject (top left) and group of controls (bottom left). (Right) Single subject z-score map.

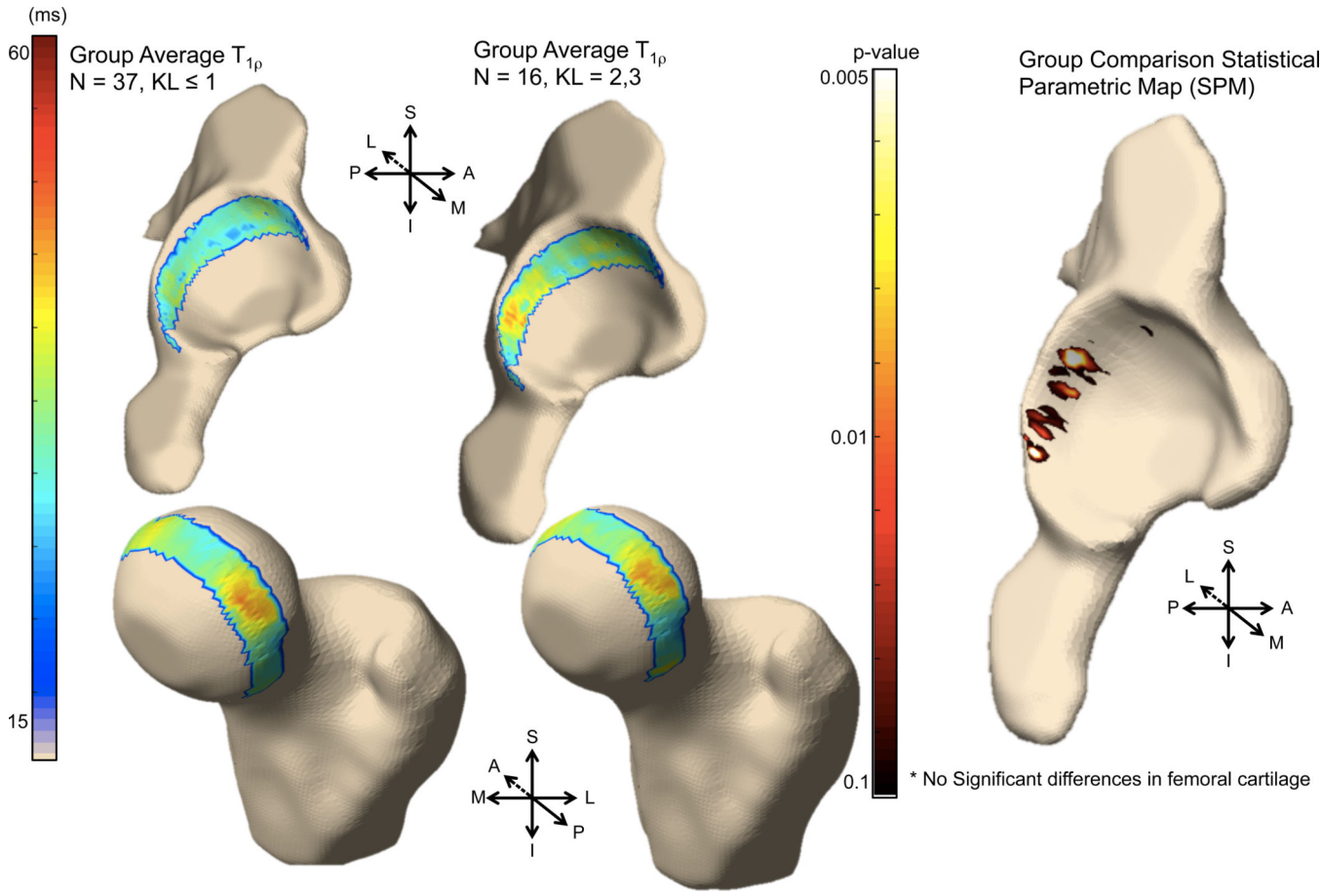

Figure 3.

3D visualization of the voxel-based $T_{1\rho}$ maps for the control (left) and OA (middle) groups. (Right) p-value statistical parametric map comparing local differences between control and OA groups.

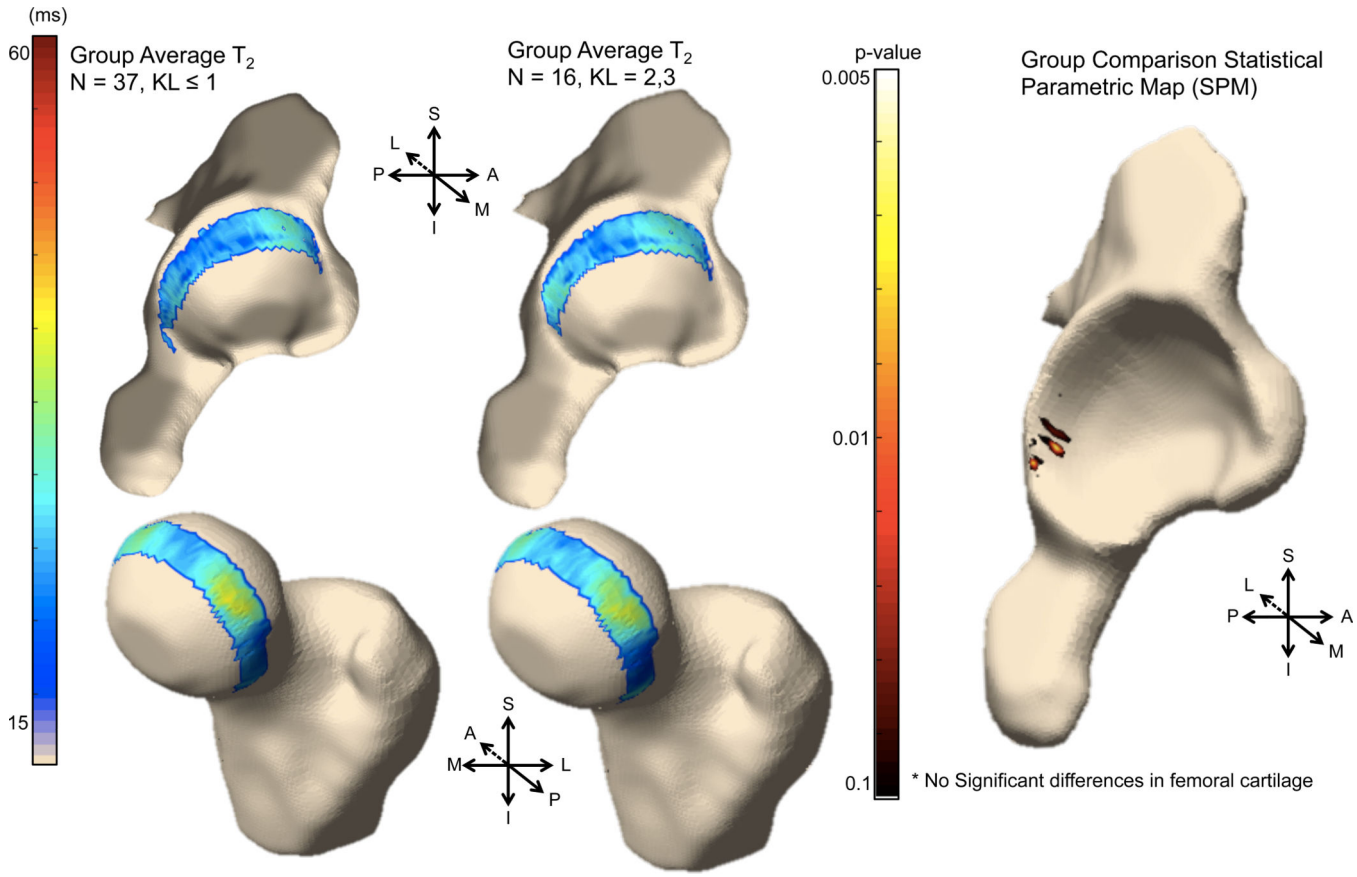

Figure 4.

3D visualization of the voxel-based T_2 maps for the control (left) and OA (middle) groups. (Right) p-value statistical parametric map comparing local differences between control and OA groups.

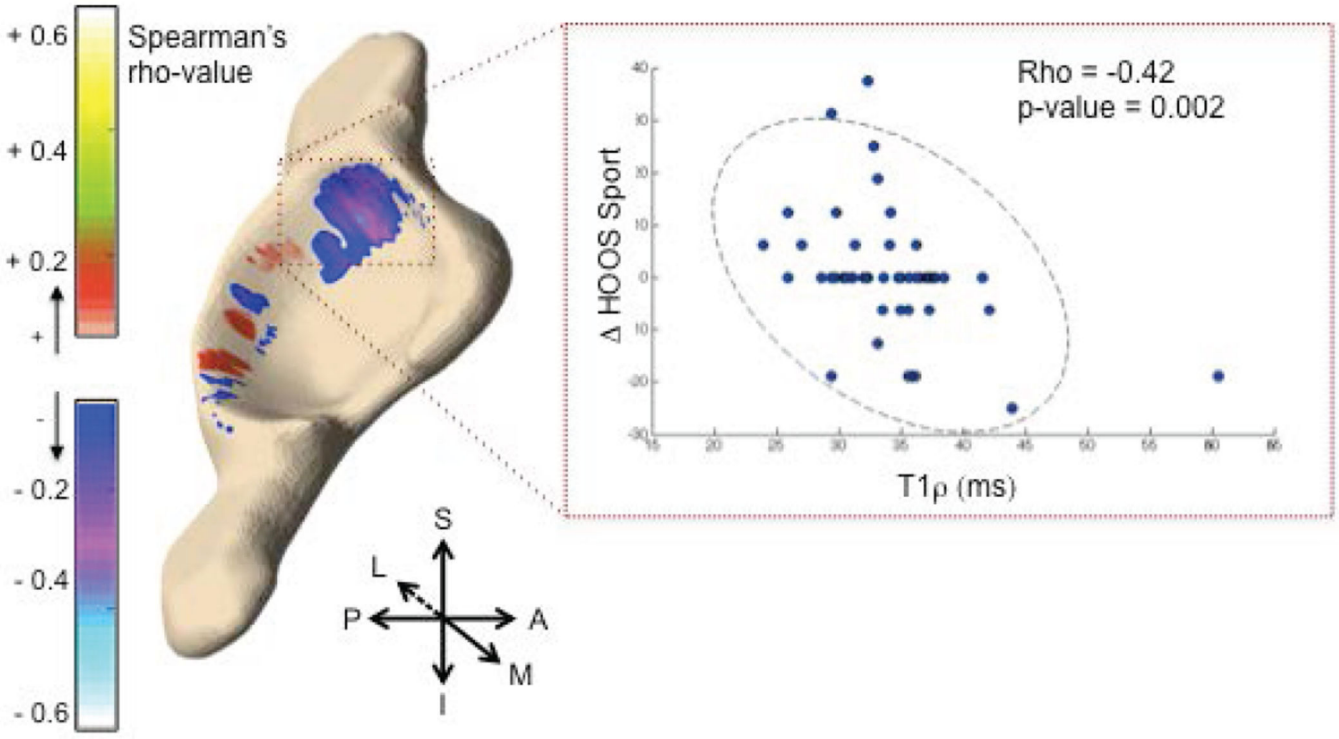

Figure 5.

3D visualization of the Spearman rho correlation map between baseline $T_{1\rho}$ and 18-month change in HOOS SPORT (left). $T_{1\rho}$ values in the anterosuperior acetabular cartilage (red box) were averaged and plotted against change in HOOS (right), showing a moderate but significant negative correlation.

Table 1

Subjects demographic and clinical characteristics (N=53)

Characteristic	KL > 1 (N=16)	KL 0–1 (N=37)	t-test
Sex[a]			
Male	10 (62.5%)	19(51.4%)	0.35
Female	6 (37.5%)	18 (48.6%)	
Age (years)[b]	53.9 ± 11.3	43.6 ± 12.8	*0.008
BMI (kg/m^2)[b]	23.8 ± 2.6	23.7 ±3.2	0.97
HOOS (0–100, 0 = worst outcome)[b]			
Pain	90.17 ± 14.88	94.58 ± 11.95	0.28
Symptoms	93.57 ± 8.64	92.22 ± 12.27	0.7
Quality of Life (SOL)	93.17 ± 11.13	95.95 ± 11.8	0.45
Sports/Recreation	91.07 ± 12.67	93.40 ± 14.32	0.59
Function in Daily Living	88.83 ± 13.46	90.27 ± 106.46	0.77

[a] Data expressed as Count (Percentage %).

[b] Data expressed as Mean ± Standard Deviation.

* significant difference between OA and control group

Table 2

MRI sequence parameters.

MRI Sequence	Sequence Parameters
3D SPGR (MERGE)	TR = 30.4 ms, 5 echo times (effective TE = 12.4 ms), flip angle = 15°, matrix = 512 × 512, 28 slices, slice thickness = 4 mm, field of view (FOV) = 14 cm, bandwidth (BW) = 62.5 kHz, NEX = 1, acquisition time 11:46 minutes
Combined $T_{1\rho}$ and T_2 (MAPPS)	FOV = 14 cm, matrix size = 256 × 128, VPS = 64, BW = 62.5 kHz, time of recovery = 1.2 sec, slice thickness = 4 mm, no gap, in-plane resolution = 0.5 mm, and acquisition time = 13:47 minutes For $T_{1\rho}$ TSL = 0/15/35/45 ms, FSL 300 Hz For T_2 TE = 0/10.4/20.8/41.7 ms

Table 3

Algorithm performance in the acetabular and femoral cartilage for the overall cohort, the control group, and the OA group. Quantification results were compared between semiautomatic and automatic approaches using coefficient of variation, absolute mean difference, and Pearson correlations.

		Semiautomatic $T_{1\rho}$	Automatic $T_{1\rho}$	Coefficient of Variation	Absolute mean difference	Semi vs Auto Pearson Corr
	ROI	mean (sd)	mean(sd)	mean (sd)	mean (sd)	(R, p-value)
Overall (n = 53)	Acetabular	33.62 (2.92)	32.98 (2.90)	2.90 (2.90)	0.64 (1.88)	0.79, < 0.001
	Femoral	36.32 (2.84)	35.35 (3.31)	2.58 (2.43)	0.98 (1.46)	0.90, < 0.001
Controls (n = 37)	Acetabular	33.37 (2.92)	32.66 (2.85)	2.56 (2.14)	0.71 (1.38)	0.89, < 0.001
	Femoral	36.27 (2.64)	35.18 (3.27)	2.76 (2.47)	1.09 (1.41)	0.91, < 0.001
Osteoarthritis (n = 16)	Acetabular	34.20 (2.93)	33.72 (2.99)	3.70 (4.15)	0.47 (2.76)	0.57. 0.022
	Femoral	36.44 (3.35)	35.73 (3.48)	2.16 (2.36)	0.71 (1.60)	0.89, < 0.001

*Radiographic definition based on Kellgren-Lawrence grade > 1 at baseline